Insertion of Filamin into Lipid Membranes Examined by Calorimetry, the Film Balance Technique, and Lipid Photolabeling†

M. Tempel,‡ W. H. Goldmann,‡ C. Dietrich,‡ V. Niggli,§ T. Weber,‖ E. Sackmann,‡ and G. Isenberg*,‡

Department of Biophysics, E22, Technical University of Munich, D-85748 Garching, FRG, Institute of Pathology, University of Bern, CH-3010 Bern, Switzerland, and Department of Biochemistry, Swiss Federal Institute of Technology (ETH), CH-8092 Zürich, Switzerland

Received May 12, 1994; Revised Manuscript Received August 8, 1994®

ABSTRACT: The interaction of the actin-binding protein filamin with mixtures of zwitterionic and anionic phospholipids (DMPC, DMPG, PC, PS) was studied in reconstituted lipid monolayers and bilayers. Protein–lipid interactions were investigated by differential scanning calorimetry, the film balance technique, and hydrophobic photoradiolabeling. For calorimetric assays, multilamellar vesicles (MLVs) and large unilamellar vesicles produced by the extrusion technique (LUVETs) were used. With MLVs, filamin induced a pronounced drop in phase transition cooperativity. Mixed DMPC/DMPG LUVETs showed a linear decrease of the main phase transition enthalpy and a significant shift in temperature for the solidus and liquidus lines with increasing mole fractions of reconstituted filamin. The insertion of native filamin into uncharged and negatively charged lipid monolayers was measured in time/area diagrams with the film balance technique. Finally, we have newly synthesized a highly sensitive lipid analogue, [^{125}]TID-PC/16, which selectively labels membrane-embedded hydrophobic domains of proteins, and which proved to label filamin, supporting evidence that this protein partially inserts into the hydrophobic domain of liposomes.

Chicken gizzard filamin and its nonmuscle analogue ABP-280 are ~160 nm elongated, highly flexible homodimers between M_r 540 000 and 580 000 with predominantly β-strand conformation (Hartwig & Stossel, 1975, 1979, 1981; Wallach et al., 1978). In its dimeric form, both proteins have actin-binding sites at each amino-terminal end and self-association sites at the carboxyl-terminal end. This renders chicken gizzard filamin as well as ABP-280 to act as efficient filament cross-linking proteins in actin gels (Nunnally et al., 1981; Cortese & Frieden, 1990; Seils et al., 1990). In nonmuscle cells, ABP-280 (nonmuscle filamin) is believed to be involved in arranging the cortical cytoplasm (Hartwig & Shevlin, 1986).

In smooth muscle cells, filamin is an abundant protein arranged in a distinct fashion in so-called surface plaques close to the plasma membrane in conjunction with vinculin and talin (Small et al., 1986; Draeger et al., 1990). Since for the latter two proteins, vinculin and talin, actin-binding and lipid interactions have been documented in vitro and in reconstituted membrane models (Niggli et al., 1986; Kaufmann et al., 1992; Isenberg & Goldmann, 1992), it appeared intriguing to investigate, in a first approach, if the actin cross-linking protein filamin would also be able to bind to lipids and to get inserted into lipid membranes directly, in vitro.

Our approach was further stimulated by the finding that filamin, when trapped in lipid vesicles (Cortese et al., 1989) or when added to vesicle suspensions (Goldmann et al., 1993), had an influence on the lipid vesicles shape, indicating that filamin might directly interact with lipid molecules arranged in a bilayer. Another hint concerning the importance of filamin–lipid interaction came from the work of Furuhashi et al. (1992), who could demonstrate that binding of filamin to micelles of phosphoinositols was inhibitory to its F-actin gelling capacity in vitro.

By using a combination of calorimetric, film balance, and photolabeling techniques, we here present substantial data that filamin directly interacts hydrophobically and electrostatically with zwitterionic and anionic phospholipids within lipid mono- and bilayers, and thus could be of importance for linking the cytoskeleton to cell membranes in vivo.

MATERIALS AND METHODS

Phospholipids. The phospholipids dimyristoyl-L-α-phosphatidylcholine (DMPC)[1] and dimyristoyl-L-α-phosphatidylglycerol (DMPG) were purchased from Avanti Polar Lipids (Birmingham, AL) and used without further purification. Phosphatidylcholine and phosphatidylserine were obtained from Lipid Products (South Nutfield, Surrey, England). Bovine serum γ-globulin was bought from Serva (Basel, Switzerland). *N*-(Texas red-sulfonyl)dipalmitoyl-L-α-phosphatidylethanolamine (Texas red DPPE) was purchased from Molecular Probes (Eugene, OR).

Buffers. Buffer reagents were purchased from Sigma (Deisenhofen, FRG). Water of Millipore quality was used for buffers. *Buffer A* consisted of 20 mM Hepes/NaOH, 1 mM EGTA, 1 mM EDTA, 0.2 mM DTT, 40 mM NaCl, and 0.005% NaN_3, pH 7.4, and was used for multilamellar vesicles (MLVs). *Buffer B* was 20 mM Hepes/NaOH, 0.3 mM

† This work was supported by Deutsche Forschungsgemeinschaft Grants DFG Is25/7-1, SFB 266/B1, and SFB 266/C5, by the Swiss National Foundation for Scientific Research (to V.N. and to Dr. J. Brunner, ETH, Zürich), by the Sandoz Foundation (Basel, Switzerland) (to V.N.), and by NATO Grant CRG 940666 to W.H.G.

* Correspondence should be addressed to this author at the Department of Biophysics, E22, Technical University of Munich, James Franck Strasse, D-85748 Garching, FRG. Fax: (49)-89-3209-2469.

‡ Technical University of Munich.

§ University of Bern.

‖ Swiss Federal Institute of Technology.

® Abstract published in *Advance ACS Abstracts,* September 15, 1994.

[1] Abbreviations: DMPC, dimyristoyl-L-α-phosphatidylcholine; DMPG, dimyristoyl-L-α-phosphatidylglycerol; Texas red DPPE, *N*-(Texas red-sulfonyl)dipalmitoyl-L-α-phosphatidylethanolamine; PC, phosphatidylcholine; PS, phosphatidylserine; MLVs, multilamellar vesicles; LUVETs, large unilamellar vesicles by the extrusion technique; DSC, differential scanning calorimetry; [^{125}]TID-PC/16, 1-palmitoyl-2-[9-[2′-[^{125}I]iodo-4′-(trifluoromethyldiazirinyl)benzyloxycarbonyl]nonanoyl]-*sn*-glycero-3-phosphocholine.

0006-2960/94/0433-12565$04.50/0

EGTA, 0.3 mM EDTA, 0.2 mM DTT, 5 mM NaCl, and 0.005% NaN_3, pH 7.4, and was used for large unilamellar vesicles produced by the extrusion technique (LUVETs).

Proteins. Filamin was isolated by the method of Shizuta et al. (1976). Low ionic strength extraction of chicken gizzard was followed by Mg^{2+} and $(NH_4)_2SO_4$ precipitations, ion exchange, and gel filtration column chromatography. For all experiments, an additional hydroxylapatite column was used to further purify the protein (Goldmann & Isenberg, 1993). The purity of filamin was checked on SDS–PAGE (cf. Figure 1) according to Laemmli (1970). The concentration of purified filamin was measured by UV spectroscopy, using an extinction coefficient of 0.82 mg^{-1} cm^{-1} at 278.5 nm (Koteliansky et al., 1982) and by the method of Bradford (1976) using ovalbumin as standard.

Lipid Vesicles and Differential Scanning Calorimetry (DSC). Lipid stock solutions were prepared by dissolving pure or mixtures of crystalline phospholipids (DMPC, DMPG) in chloroform/methanol, 2/1 (v/v). From aliquots of these solutions, a dry lipid film was formed on the walls of an extensively rinsed glass beaker by evaporating the solvent with a stream of nitrogen followed by vacuum desiccation for at least 2 h. For the preparation of multilamellar vesicles (MLVs), the lipid film was first redispersed in buffer A by repeated vortexing and then equilibrated overnight at 42 °C.

Large unilamellar vesicles (LUVETs) produced by the extrusion method at diameters ≤100 and ≤200 nm were formed by homogenization of MLVs (Hope et al., 1985). Briefly, the dry lipid film was taken up in buffer B followed by five cycles of freeze/thawing to generate MLVs. Then the lipid dispersion was pressed 10 times through two (stacked) 100 or 200 nm Nucleopore polycarbonate filters of an extruder (Lipex, Canada). Vesicles ≤400 nm in size were produced by fusion of 100 nm LUVETs stored for 48 h at 4 °C (Wong et al., 1982). All extrusion procedures were conducted at least 10 °C above the gel–liquid-crystal transition temperature. Vesicle solutions were slightly turbid. The mean diameter of the size- and mass-weighted vesicle distribution of 100 nm DMPC LUVETs was judged from freeze–fracture EM micrographs as 74 ± 22 nm (mean value ± SD) (Schullery et al., 1980).

Samples were equilibrated at 4 °C for 30 min. Calorimetric measurements were carried out in a Microcal MC-2 unit (Microcal Inc., Amherst, MA). DSC samples (1.5 mL) containing 0.5–2.8 mg of lipids were injected into the sample cell, and scans were performed at a rate of 30 °C/h. Data were collected at 0.05 °C intervals. Thermograms were stored on an IBM AT computer. After the measurements, quantification of the phospholipid content of the sample was achieved by the "macro assay phosphorous method" (Zhou & Arthur, 1992) to a precision of 2.5%.

The transition enthalpy, ΔH, of a normalized and base-line-corrected thermogram was calculated as the numerically integrated area below the endotherm (Note: the base line was determined by defining in the endotherm two base line information containing regions, where one region was located below and the other region above the examined phase transition, and then the regions were connected by a second-order polynomial curve). The phase transition temperature, T_m, was defined as the temperature at which the excess specific heat reaches a maximum. The sharpness of the transition was expressed as the temperature width at half-maximum height, $\Delta T_{1/2}$. To describe the width of the gel to liquid-crystalline transition of lipid mixtures, the onset temperature of chain melting, T_s, which represents the solidus line, and the completion temperature of chain melting, T_l, which represents the liquidus line, were determined. T_s and T_l were defined as those temperatures where the integration over the heat capacity function resulted in 0.3% and 99.7% of the total transition enthalpy, respectively.

Filamin was reconstituted into preformed MLVs or LUVETs by repeated cycles of heating/cooling between 4 and 37 °C. This procedure prevented thermal denaturation of filamin which starts at ~40 °C (Koteliansky et al., 1982). The heating/cooling cycles were carried out with the DA2 microcalorimeter at a scan rate of 30 °C/h. This method allowed a direct observation of the influence of filamin on the lipid phase transitions. The samples were rescanned 6 times. In contrast to measurements with pure lipids, for measurements with filamin/lipid mixtures clearly visible differences could be detected between the first and subsequent scans. After the second to fifth heating scan, the heat capacity profiles became identical, indicating that the reconstituted lipid/protein system was at equilibrium.

Lipid Monolayers and Film Balance Measurements. The phospholipids DMPC or DMPG were dissolved in a chloroform/methanol solution of 9/1. To allow observation by epifluorescence microscopy, Texas red DPPE was added to the unlabeled lipids at a molar ratio of 1/1000. If not otherwise stated, these lipids were then spread onto a solution, containing 10 mM Hepes, pH 7.4, at various salt concentrations (0–150 mM NaCl), rendering a homogeneous lipid monolayer.

Monolayer experiments were performed with a film balance apparatus developed by Heyn et al. (1991) and described in detail by Dietrich et al. (1993). In short, this unit consists of a fluorescence microscope which is placed above a Langmuir trough. The microscope is mounted on a motorized "x–y" translation stage to allow observation of the fluid surface. The base of the 30 mL trough is brass-plated, and Peltier elements are used underneath for temperature regulation (accuracy ~0.2 °C). Most parts of the trough are covered by a glass slide to protect a spread lipid monolayer from impurities, air convection, and fluid condensation. The surface pressure of solutions in the trough is measured by a Wilhelmy system. Pressure/area diagrams of lipid monolayers are obtained by isothermal compression and expansion. Time scans recorded at constant pressure for recording the area or at constant area for recording the pressure were performed. The scanning speed of the film balance apparatus and the process of recorded lateral pressure measurements are controlled by an IBM-compatible PC-AT.

Hydrophobic Photolabeling and Evaluation. [^{125}I]TID-PC/16, 1-palmitoyl-2-[9-[2′-[^{125}I]iodo-4′-(trifluoromethyldiazirinyl)benzyloxycarbonyl]nonanoyl]-*sn*-glycero-3-phosphocholine, was prepared as described by Weber and Brunner (1994) with a specific activity of 2 × 10^3 Ci/mmol.

[^{125}I]TID-PC/16-containing liposomes were prepared as described by Goldmann et al. (1992). The liposomes in 20 mM Hepes and 0.2 mM EGTA, pH 7.4, consisted either of phosphatidylserine or of phosphatidylcholine and of 0.001% (w/w of total lipid) [^{125}I]TID-PC/16. Proteins were dialyzed against 20 mM Tris-HCl, pH 7.4, 0.1 mM EDTA, and 15 mM mercaptoethanol prior to experimentation. As a control, bovine serum γ-globulin (mainly IgG) was dialyzed against this buffer lacking mercaptoethanol. Photolysis, SDS–polyacrylamide gel electrophoresis (SDS–PAGE), and autoradiography of the protein–lipid mixtures were carried out as described by Goldmann et al. (1992).

For quantification of labeling, protein-containing slices were cut out from Coomassie Blue-stained 5–10% gradient gels,

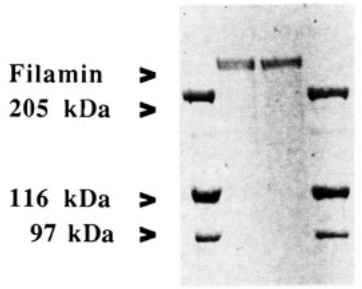

FIGURE 1: 6.5% SDS–PAGE gel showing the purified protein filamin taken from the gel filtration column. Molecular mass standards are indicated by numbers; 5 μg of protein was loaded per lane.

placed into 3 mL plastic tubes, and counted in a Packard crystal 5400 γ counter. Background counts per minute (cpm) obtained in the same lane were subtracted from the cpm of the protein-containing slices. To correct for unequal protein loading, the amount of protein in the bands was evaluated by scanning the Coomassie blue-stained gels and compared with defined amounts of talin, vinculin, and filamin, respectively. The staining intensity was linear in the range of 2–8 μg of protein.

RESULTS

Purified filamin from smooth muscle (Figure 1) was used in all experiments.

Differential Scanning Calorimetry

Influence of Filamin on Phase Transitions of MLVs. The change of the excess specific heat with rising temperature for pure DMPC (MLVs) and DMPC (MLVs) in the presence of increasing filamin concentrations is shown in Figure 2A, curves a–d, representing the pre-phase transition, and in Figure 2B, curves a–d, representing the main phase transition. All traces are normalized concerning the lipid concentration in the measuring cell and corrected by the same base line for direct comparison.

For pure DMPC MLVs (control system), the values of ΔH = 0.85 ± 0.10 kcal/mol with T_m = 13.4 ± 0.1 °C for the pretransition and ΔH = 6.30 ± 0.15 kcal/mol with T_m = 23.8 ± 0.1 °C are in good agreement with reported data (Parente & Lentz, 1984). With increasing filamin concentrations (protein/lipid molar ratio from 0 to 1/170), the pretransition enthalpy was significantly reduced to approximately 25% of the value compared to pure DMPC, and the main transition temperature (T_m) was changed only negligibly with a small decrease in transition enthalpy from ΔH = 6.30 ± 0.15 kcal/mol for pure lipids to ΔH = 5.95 ± 0.15 kcal/mol at a 1/170 protein/lipid molar ratio. These results—with respect to enthalpy reduction—can be interpreted in terms of conformationally inhibited lipid molecules adjacent to bound filamin which therefore are unable to undergo a phase transition [cf. Lentz et al. (1985)].

As shown in Figure 2B, the effect of filamin on the thermotropic properties of lipid molecules consists of a shift of the chain melting "onset temperature", T_s (solidus line), to lower temperatures, giving the entire phase transition profile an asymmetric contour. In general, when proteins and lipids interact, the low-temperature shift of the solidus line, T_s, is assigned to hydrophobic interactions. At the highest protein/lipid molar ratio, 1/170, the difference between T^*_s (solidus line in the absence of proteins) and T_s (solidus line in the presence of proteins) equals ~1.0 °C. The small value of this shift is indicative for a weak hydrophobic interaction of filamin

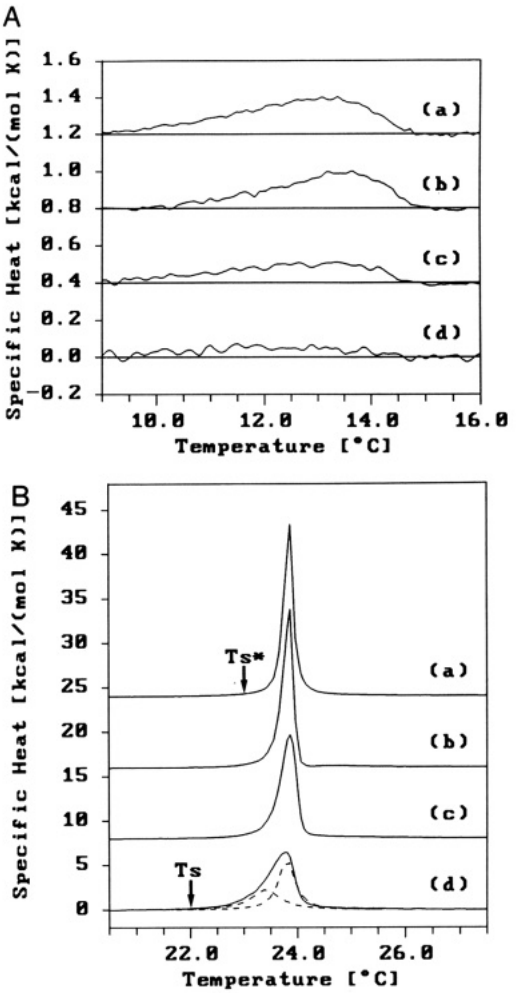

FIGURE 2: DSC heating profiles of pure and filamin-reconstituted DMPC MLVs. The endotherms in panels A and B show the variation of the pre- and main-phase transition, respectively, with increasing concentrations of filamin. The incubation protein/lipid molar ratios of the endotherms were (a) P/L = 0 (pure lipid), (b) P/L = 1/670, (c) P/L = 1/320, and (d) P/L = 1/170. The scans are normalized to the mass of phospholipid, and the base line is corrected. For the main phase transition at the protein/lipid ratio 1/170 (panel B, curve d), the dashed lines represent the deconvolution of the endotherm into a sharp and a broad component, centered at the transition temperatures T_m = 23.8 °C and T_m = 23.4 °C, respectively. In all experiments, *buffer A* (20 mM Hepes/NaOH, 1 mM EGTA, 1 mM EDTA, 0.2 mM DTT, 40 mM NaCl, and 0.005% NaN_3, pH 7.4) was used.

with the DMPC MLVs. The asymmetric contour of the phase transition profile at a protein/lipid molar ratio of 1/170 as shown in Figure 2B, curve d, can be divided—when deconvoluted—into a sharp, T_m = 23.8 °C, and a broad, T_m = 23.4 °C, component (both in dashed lines). The sharp component shows transition characteristics of pure lipids, while the broad component at the lower T_m is indicative for a markedly increased transition width as compared to protein-free DMPC. The decrease in sharpness of the main phase transition suggests a disruption of the cooperative behavior of the lipid matrix. A relative measure for the cooperativity of lipid systems is the value of the half-width, $\Delta T_{1/2}$, of the phase transition [cf. McElhaney (1986)]. To compare the widths, $\Delta T_{1/2}$, of vesicle systems composed of different phospholipids, we defined the term "relative widening":

$$\text{relative widening} = (\Delta T_{1/2} - \Delta T^*_{1/2})/\Delta T^*_{1/2}$$

where $\Delta T^*_{1/2}$ is the width at half-height of the main transition

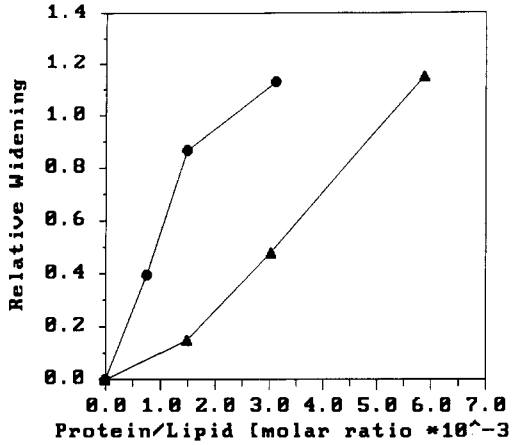

FIGURE 3: "Relative widening" $[(\Delta T_{1/2} - \Delta T^*_{1/2})/\Delta T^*_{1/2}]$ determined from DSC profiles for the main-phase transition of DMPC MLVs (▲) and DMPC/DMPG 50/50 MLVs (●) plotted as a function of various incubation filamin/lipid molar ratios.

in the absence of protein and $\Delta T_{1/2}$ is the width at half-height of the main transition in the presence of protein. In Figure 3, the calculated values of the relative widening for protein–lipid systems of different lipid mixtures were used and plotted against various protein/lipid molar ratios: DMPC (▲) taken from Figure 2B and DMPC/DMPG (●) at a ratio of 50/50 (endotherms not shown). As shown in Figure 3, the calculated values for the relative widening are >0. This means that the cooperative behavior of the lipids—independent of the lipid composition—is less pronounced in the presence of filamin. Data obtained from DMPC proteovesicles (in the presence of filamin) clearly show a disturbing influence of filamin on lipid packing and order, indicating a partial incorporation of the protein into the lipid bilayer. Data obtained from DMPC/DMPG (50/50) (●) vesicles reveal that in the presence of anionic phospholipids this disturbing effect of filamin on the chain melting behavior is further enhanced, indicating the existence of additional forces either purely electrostatic in nature or consisting of electrostatic and hydrophobic moments.

Influence of Filamin on Phase Transitions of LUVETs. The interaction between filamin and LUVETs composed of pure phospholipid (DMPC) versus mixed phospholipids (DMPC/DMPG 70/30 and 50/50, w/w) was also examined by differential scanning calorimetry. In contrast to the results obtained for MLVs (see above), filamin caused only negligible changes of the chain melting process in pure DMPC LUVETs. The width and position of the main phase transition were not influenced, but a small continuous loss of transition enthalpy with increasing protein mole fraction could be detected (cf. Figure 6A). With DMPC/DMPG (70/30) and DMPC/DMPG (50/50) LUVETs, however, reconstituted filamin resulted in a strong disturbance of the thermotropic behavior of lipids. Representative DSC thermograms of DMPC/DMPG 50/50 LUVETs at various lipid/protein molar ratios (ranging from protein/lipid molar ratios of 1/2080 to 1/420) are shown in Figure 4. Data are corrected as in Figure 2.

Transition profiles of LUVETs without protein show a "tailing off" toward the low-temperature side of the heat thermogram, giving rise to an entire asymmetric contour. This behavior suggests the existence of fractions with small- and intermediate-sized unilamellar vesicles (diameters 30–60 nm) with a transition temperature, T_m, lower than those of large unilamellar vesicles (Lentz et al., 1987). Further, separate peaks indicate a nonideal miscibility of the lipids DMPC and DMPG at low-salt buffer conditions. [Note: If DMPC/DMPG 50/50 LUVETs were prepared in high-salt buffer

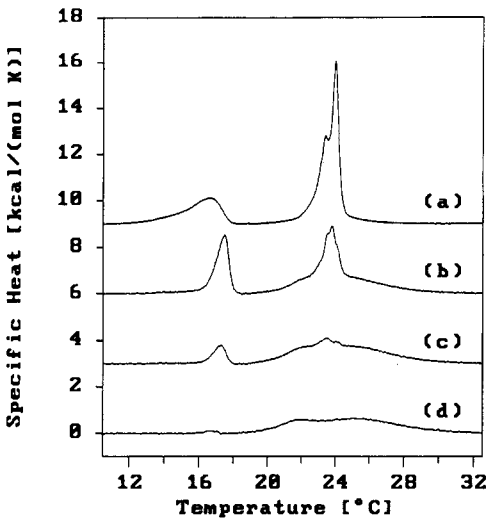

FIGURE 4: DSC profiles of pure and filamin-reconstituted DMPC/DMPG 50/50 LUVETs. The endotherms show the variation of the pre- and main-phase transition with increasing concentrations of filamin (a–d). The incubation molar ratios of protein/lipid were (a) $P/L = 0$ (pure lipid), (b) $P/L = 1/2080$, (c) $P/L = 1/1010$, and (d) $P/L = 1/420$. The scans are normalized to the mass of phospholipid, and the base line is corrected. *Buffer B*: 20 mM Hepes/NaOH, 0.3 mM EGTA, 0.3 mM EDTA, 0.2 mM DTT, 5 mM NaCl, and 0.005% NaN_3, pH 7.4.

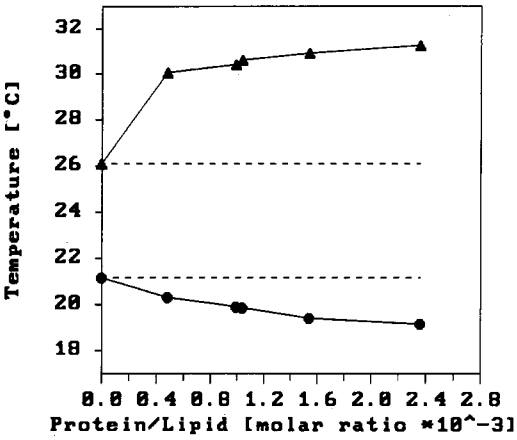

FIGURE 5: T_s (solidus line; ●) and T_l (liquidus line; ▲) as a function of various protein/lipid molar ratios. DMPC/DMPG 50/50 LUVETs were incubated with rising filamin concentrations. The temperatures T_s and T_l were calculated from heat capacity profiles as partially shown in Figure 4.

(500 mM NaCl), the heat capacity profile exhibited a smooth asymmetric end at lower temperatures]. Incorporation of filamin produces notable changes in the shape and enthalpy of the pre- and main-phase transition. The pre-transition of the protein-free lipid mixture is shifted and gradually suppressed with increasing filamin concentrations. In comparison to the main-phase transition obtained with pure lipids, the formation of a low- and a high-temperature shoulder and an enthalpy reduction can be recognized. This is qualitatively very similar to the interaction of talin with unilamellar DMPC/DMPG 50/50 vesicles (Heise et al., 1991).

The incubation of DMPC/DMPG LUVETs with filamin significantly shifts the onset of the chain melting temperature, T_s (solidus line), to lower temperatures and the completion of the chain melting temperature, T_l (liquidus line), to higher temperatures. Figure 5 shows the onset and completion temperatures for DMPC/DMPG 50/50 LUVETs in relation to the protein/lipid molar ratio. The chain melting transition was shifted from $T_{l^*} - T_{s^*} = 4.9$ °C in protein-free vesicles to

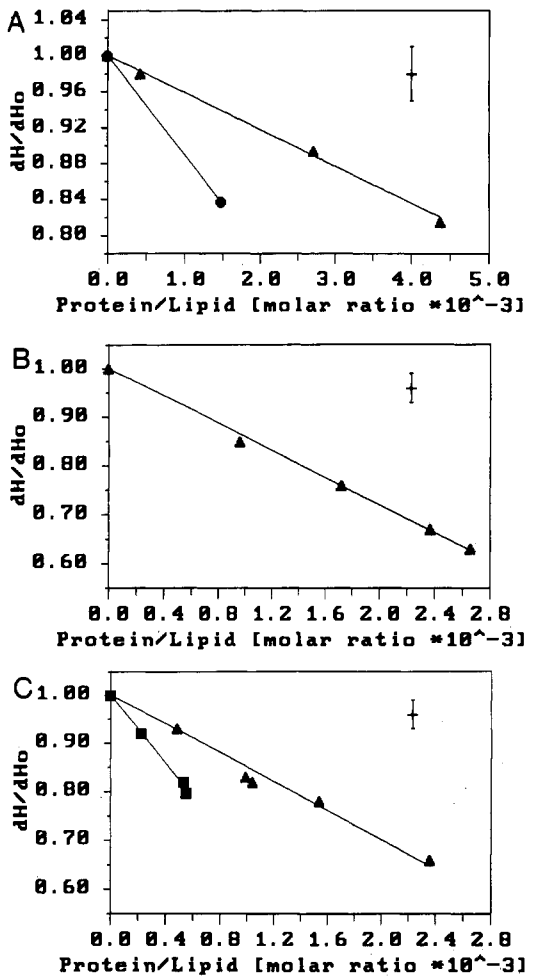

FIGURE 6: Relative decrease in transition enthalpy, $\Delta H/\Delta H_0$, plotted for the main-phase transition of large unilamellar vesicles with 100 (▲), 200 (■), and 400 nm (●) diameter as a function of increasing filamin/lipid molar ratios. The lipid compositions were (A) DMPC (ΔH_0 = 6.55 ± 0.20 kcal/mol), (B) DMPC/DMPG 70/30 (ΔH_0 = 7.00 ± 0.20 kcal/mol), and (C) DMPC/DMPG 50/50 (ΔH_0 = 7.15 ± 0.20 kcal/mol). The straight lines represent the best fit to the data with a y-intercept equal to unity. The slopes, which give the number of boundary lipid molecules per protein molecule, were calculated as follows: (A) (▲) = 41 ± 3; (B) (▲) = 140 ± 5; (A) (●) = not done; (C) (▲) = 150 ± 10; (C) (■) = 355 ± 15. The error bars are representative for the error of each data point and result from the accuracy of the quantitative phospholipid determination of 2.5%. Note: An error in the average numbers, $\langle n \rangle$, could result from the plot of enthalpy *vs* protein/lipid molar incubation ratios. It is assumed that all filamin molecules bound to the lipid as well as the vesicle population are homogeneously affected by the protein/lipid interaction. The $\langle n \rangle$ values should primarily serve to estimate the dimension of effects observed.

$T_1 - T_s$ = 9.8 °C at the lowest protein/lipid molar ratio of 1/2080. At a protein/lipid molar ratio of 1/420, the main transition broadened to $T_1 - T_s$ = 12.1 °C, indicating saturation behavior with increasing protein concentrations.

The relative decrease in transition enthalpy, $\Delta H/\Delta H_0$ (ΔH_0, lipid main transition enthalpy in the absence of protein), as a function of rising filamin/lipid ratios is plotted for various lipid compositions in Figure 6A–C. For all tested lipid compositions, the transition enthalpy decreases linearly with increasing protein/lipid ratios, indicating that filamin prevents a fraction of the phospholipid molecules from undergoing chain melting. The data can be fitted quite well by a straight line according to the equation:

$$\Delta H/\Delta H_0 = 1 - \langle n \rangle (P/L)$$

Table 1

protein concn (μg/mL)	pressure (mN/m)
55 ± 5	15.5 ± 3
11 ± 1	12.5 ± 2
2.2 ± 0.3	15.5 ± 2
0.55 ± 0.2	5 ± 4

where, $\langle n \rangle$ is the average number of boundary lipid molecules per protein molecule and P/L is the protein/lipid molar ratio (Correa-Freire et al., 1979). Least-squares fits of data using this equation and a y-intercept equal to unity gave the following values for the slope, $\langle n \rangle$: 41 ± 3 (DMPC), 140 ± 5 (DMPC/DMPG 70/30), and 150 ± 10 (DMPC/DMPG 50/50) for LUVETs with 100 nm diameter (▲) (Figure 6A–C). These data imply that the effect of filamin on the transition energy of the chain melting process is enhanced in the presence of the anionic lipid DMPG.

Enthalpy changes using fusionated DMPC vesicles with 400 nm diameter (●) (Figure 6A) and DMPC/DMPG (50/50) LUVETs with 200 nm diameter (■) (Figure 6C) were also examined. When comparing the $\langle n \rangle$ values of DMPC/DMPG (50/50) vesicles with 100 and 200 nm diameter, approximately twice as much lipid is excluded to undergo a phase transition in the 200 nm vesicles. For the 400 nm filamin–DMPC vesicles, also a pronounced enthalpy decrease was detected.

To control for the specificity of filamin–lipid interactions as measured by DSC, filamin was denatured first by heating the protein for 60 min up to 100 °C. Subsequent incubation with DMPC/DMPG 50/50 LUVETS rendered a marked reduction in hydrophobic and electrostatic interactions as indicated by a smaller shift of T_s and T_1 of the main phase transition as well as a less pronounced reduction of ΔH (data not shown).

Insertion of Filamin into Lipid Monolayers As Measured by the Film Balance Technique

Before monitoring the insertion of filamin into lipid monolayers, we measured the surface tension of protein solutions at the liquid–air interface in the absence of lipids. A buffer containing 10 mM Hepes, 10 mM NaCl, pH 7.5, was used into which filamin was injected. Due to protein enrichment at the liquid–air interface, the surface pressure is induced (Graham & Philips, 1979). The pressures shown in Table 1 were measured after protein injection. The interaction of the protein with the liquid–air interface is only possible at a lateral pressure ≤15 ± 3 mN/m.

To avoid an artificial interaction of filamin with the air–water interface when using lipids, all experiments were performed at a pressure of 25 mN/m, which was significantly higher than the equilibrium pressures listed in Table 1.

Time/Area Diagrams. The film balance apparatus allows the recording of time/area diagrams of lipid monolayers at constant pressure. All lipid monolayers at thermodynamic equilibrium normally show a constant area with time. Figure 7 displays the effect of various salt concentrations when 17 μg/mL filamin is injected (marked by arrow) into the subphase of pure DMPG monolayers. In subsequent experiments, the pressure for all lipids—spread onto the buffer surfaces—was kept constant at 25 mN/m and 20 °C. At high salt (150 mM NaCl), the presence of filamin shows a negligible influence in area compared to a marked increase in area at low salt (10 mM NaCl). However, dependent on the salt concentration,

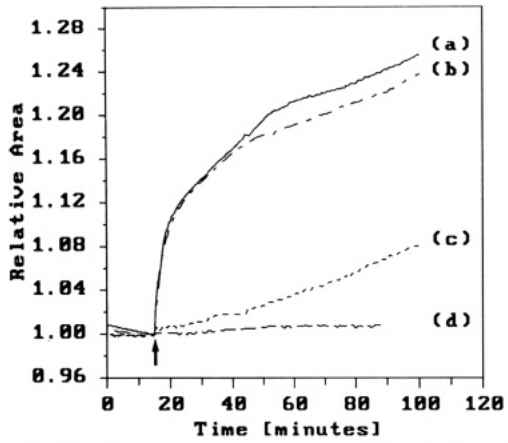

FIGURE 7: Time/area diagram as measured by the film balance technique. DMPG phospholipid monolayers were incubated with 17 μg/mL filamin at various buffers as subphase: (a) 10 mM Hepes, pH 7.6, 20 °C, with no NaCl; (b) with 10 mM NaCl; (c) with 40 mM NaCl; (d) with 150 mM NaCl. The arrow marks the injection of filamin into the subphase. The pressure of 25 mN/m was kept constant in all monolayer measurements.

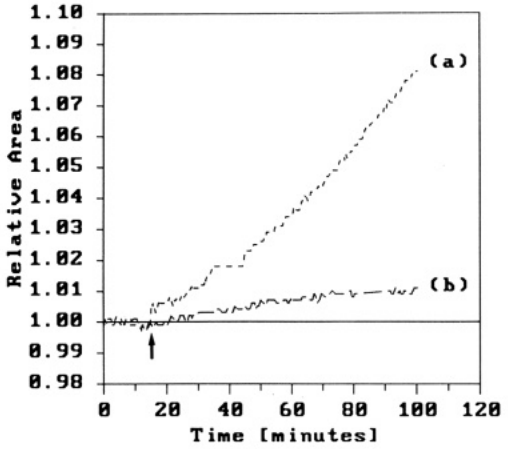

FIGURE 8: Time/area diagram as measured by the film balance technique. Pure DMPG and pure DMPC phospholipid monolayers after injection of 17 μg/mL filamin into the subphase: (a) 10 mM Hepes, pH 7.6, 20 °C, 40 mM NaCl for DMPG; (b) 10 mM Hepes, pH 7.6, 20 °C, 10 mM NaCl for DMPC. The straight line represents pure lipid systems. The arrow marks the injection of filamin into the subphase. The pressure of 25 mN/m was kept constant in all monolayer measurements.

different monolayer morphologies are detected by fluorescence microscopy (Lösche et al., 1983; Weiss & McConnel, 1984). At NaCl concentrations ≥40 mM, DMPG at 25 mN/m is in the LE-phase (liquid-expanded phase). At low salt concentrations, ≤10 mM NaCl, DMPG is in coexistence between the LE and the LC (liquid-condensed) phase.

In addition, we have tested the incorporation of filamin into lipid monolayers depending on the lipid composition. Figure 8 represents experiments with pure DMPG at 40 mM NaCl (a) and with DMPC at 10 mM NaCl (b) which were performed as described above. The filamin subphase concentration was again 17 μg/mL. Results show that a pronounced anionic charge potential of the lipid headgroups or subphase surface is obviously necessary to induce filamin insertion into the lipid monolayer.

Hydrophobic Photolabeling

Hydrophobic photolabeling of filamin was compared to that of vinculin and talin, proteins known to insert into bilayers containing acidic phospholipids (Goldmann et al., 1992). As

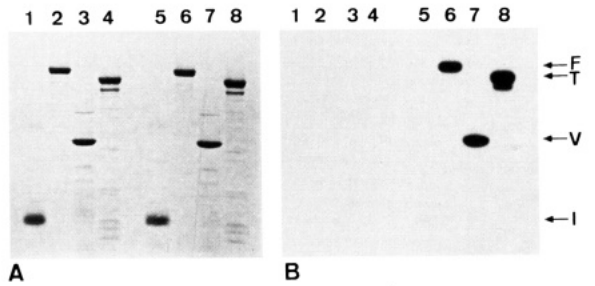

FIGURE 9: Hydrophobic photolabeling of filamin in the presence of phosphatidylcholine- or phosphatidylserine-containing liposomes compared to that of talin and vinculin. Proteins were preincubated in the absence of liposomes for 15 min at room temperature. Liposomes containing trace amounts of [^{125}I]TID-PC and either phosphatidylcholine (lanes 1–4) or phosphatidylserine (lanes 5–8) were then added to the proteins, and incubation was continued for a further 15 min. Final concentrations: lipid = 0.5 mg/mL, protein = 0.15 mg/mL. Subsequently, the samples were photolyzed and analyzed by SDS–PAGE and autoradiography. Bovine IgG was treated in the same way as the control. Five micrograms of protein was applied per lane. (A) Coomassie Blue-stained 5–10% gradient gel; (B) the corresponding autoradiogram. Lanes 1–5, bovine IgG; lanes 2–6, filamin; lanes 3–7, vinculin; lanes 4–8, talin. Arrows indicate the positions of filamin (F), vinculin (V), talin (T), and the heavy chain of IgG (*t*).

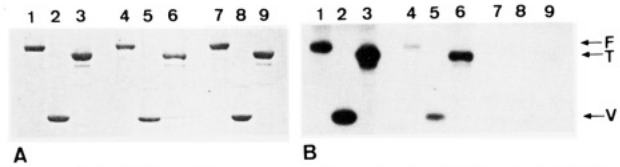

FIGURE 10: Effect of ionic strength on hydrophobic photolabeling of filamin, talin, and vinculin. Proteins were incubated with phosphatidylserine liposomes containing trace amounts of [^{125}I]TID-PC, photolyzed, and subjected to SDS–PAGE and autoradiography as described in the legend (Figure 8). 5 μg of protein was applied per lane. (A) Coomassie Blue-stained 5–10% gradient gel; (B) the corresponding autoradiogram. Lanes 1, 4, 7, filamin; lanes 2, 5, 8, vinculin; lanes 3, 6, 9, talin. Lanes 1–3, proteins were photolyzed in the presence of phosphatidylserine liposomes, but in the absence of added salt. Lanes 4–6, proteins were photolyzed in the presence of phosphatidylserine liposomes and in the presence of 260 mM KCl and 2 mM $MgCl_2$. Lanes 7–9, proteins were incubated in the presence of phosphatidylserine liposomes, but with no salt added and without photolysis. Arrows indicate the positions of filamin (F), talin (T), and vinculin (V).

shown in Figures 9 and 10, filamin indeed was also labeled under the same conditions similar to those of vinculin and talin. Filamin labeling was dependent on the presence of acidic phospholipids (Figure 9, lanes 2+6) and was decreased, but not abolished, by increasing the ionic strength (Figure 10, lanes 1+4). Labeling was completely abolished when photolysis was omitted (Figure 10, lane 7) or when the liposomes contain only phosphatidylcholine and trace amounts of photolabel (Figure 9, lane 2). Specific filamin labeling was reproducibly lower under all conditions tested compared to talin and vinculin but was still significantly higher than that of a control protein, bovine IgG. Specific labeling of filamin in the presence of phosphatidylserine liposomes, but in the absence of added salt, amounted to 320 ± 130 cpm per 5 μg (mean ± SD, $n = 3$). For comparison, talin incorporated 800 ± 150 cpm per 5 μg and vinculin 560 ± 140 cpm per 5 μg under the same conditions. In the presence of 160 mM KCl and 1 mM $MgCl_2$, labeling of filamin was reduced to 24–25% of the value obtained in the absence of added salt (talin to 76–94%; vinculin to 64–78%). Under optimal conditions, filamin incorporated 0.04–0.13% of the total radioactivity (vinculin, 0.1–0.16%; talin, 0.18–0.24%). The control protein IgG incorporated, in the presence of phosphatidylserine

liposomes and in the absence of added salt, 50–100 cpm per 5 μg of protein (0.01–0.03% of total radioactivity). Filamin incorporated in three different experiments always about 4 times more radioactivity compared to the control protein IgG. The data obtained for specific labeling of vinculin and talin correspond very well with data previously shown for these proteins with another photolabel of very similar structure, [^{3}H]PTPC/11 (Goldmann et al., 1992).

DISCUSSION

The role of the lipid interaction in the function of actin-binding proteins is of particular interest, since more and more proteins are known which share this capability [for a review, cf. Isenberg (1991), Janmey (1994), and Isenberg and Goldmann (1995)]. Lipid binding of actin-associated proteins is not as unspecific as initially thought: e.g., binding of the actin cross-linking and lipid-binding protein α-actinin (Jockusch & Isenberg, 1981; Fritz et al., 1993) to actin is enhanced by PIP-2 whereas the actin cross-linking activity of chicken gizzard filamin is suppressed (Furuhashi et al., 1992). In general, the anchorage of actin cross-linking proteins to the plasma membrane is believed to be of crucial importance for stabilizing the cortical cytoplasmic actin filament network within cells.

Differential scanning calorimetry has proved to be a valuable method for measuring lipid phase transitions by giving information about the packing and order of lipids with respect to temperature. Hydrophobic and/or electrostatic changes due to protein–lipid interactions can be detected by this accurate method.

To elucidate the potential interactions of the actin filament cross-linking protein filamin with lipid bilayers and monolayers, we have chosen different vesicle systems of various lipid compositions. Multilamellar vesicles (MLVs) and large unilamellar vesicles produced by the extrusion technique (LUVETs) were used because of the following alternative advantages: MLVs give rise to very sharp main phase transitions, allowing the detection of subtle perturbations during the lipid melting process. However, MVLs have some disadvantages: First, the heterogeneity in size (diameters ranging from 0.1 to several micrometers) does not easily allow a correlation between bilayer curvature and protein incorporation. Second, due to the multiple lipid layers, changes of the transition enthalpy at various protein to lipid ratios cannot be interpreted in a quantitative way. We have used LUVETs alternatively, since these vesicles offer a solution to the mentioned problems.

Our results obtained by differential scanning calorimetry clearly show that filamin interacts with phospholipids. The nature of filamin–lipid interactions depends on the type of phospholipid. For pure, uncharged DMPC vesicles, we found that filamin suppresses the enthalpy of the pre-phase transition and broadens the main phase transition. These effects, though small, are indicative of a weak hydrophobic interaction. The addition of negatively charged phospholipids results in a drastic reduction of the pre-phase transition, a significant decrease in the main phase transition enthalpy, and a marked shift of the solidus and liquidus lines. These shifts are most readily explained by two effects: First, a hydrophobic interaction due to a partial penetration of amino acid side chains into the lipid bilayer core which expands, destabilizes, and rearranges the phospholipid structure will give rise to lipid phases with transition temperatures lower than those obtained for pure lipids. Second, an electrostatic, charge-neutralizing interaction occurring at the membrane surface, condensing and stabilizing the gel phase of the phospholipid bilayer, will give rise to lipid phases with transition temperatures higher than those of the pure lipids. These effects could lead to an electrostatic attachment and hydrophobic insertion of filamin into charged phospholipid bilayers. Using LUVETs of different sizes, we also observed that the filamin–lipid interaction depends on the vesicle surface curvature.

The same type of filamin–lipid interaction was demonstrated by film balance analyses: at low salt concentrations, only a small surface increase is measurable after insertion of filamin into uncharged DMPC lipid monolayers, whereas a rapid and pronounced surface increase—due to insertion—is observed as soon as negatively charged phospholipids are present in the lipid monolayer. However, this marked effect is suppressed in the presence of high salt.

For hydrophobic labeling, we have synthesized a new photoactivatable, highly sensitive lipid analogue, [^{125}I]TID-PC/16, which selectively reacts with hydrophobic membrane-embedded domains of proteins. Probably due to a relatively low labeling efficiency, the insertion of filamin into pure, uncharged PC liposomes was undetectable by this method. Labeling, however, was significantly increased in the presence of negatively charged phospholipids. Hydrophobic labeling occurred in a comparable manner as with the actin- and lipid-binding proteins talin (Goldmann et al., 1992) and vinculin (Niggli et al., 1986). However, when compared with talin, the labeling efficiency for filamin was approximately 3-fold lower.

Interestingly, hydrophobic lipid photolabeling of filamin, in contrast to vinculin and talin, was much more reduced in the presence of salt (260 mM KCl, 2 mM $MgCl_2$) which opens the possibility that the filamin–membrane interaction in vivo may be more sensitive to regulation by ionic strength.

In summary, we have presented evidence by three independent approaches that filamin in vitro interacts with phospholipids hydrophobically and electrostatically and can be reconstituted into lipid vesicle bilayers as well as into lipid monolayers. Our monolayer studies further allow the conclusion that filamin hydrophobically inserts into one half of the membrane leaflet rather than spanning the whole lipid bilayer. For nonmuscle filamin, a highly hydrophobic α-helical segment of the primary sequence (residues 136–154) could be identified by computer analyses and structure predictions (Tempel et al., 1994), sufficient to allow anchoring in the hydrophobic domain of lipid membranes. In light of the fact that filamin is regulated in its function by phosphoinositols (Furuhashi et al., 1992), the described interaction with phospholipid membranes is of particular interest.

ACKNOWLEDGMENT

We thank Ms. H. Kirpal and Ms. K. Mujynya-Ludunge for excellent technical assistance and Ms. C. Meissner for careful reading.

REFERENCES

Bradford, M. (1976) *Anal. Biochem. 72*, 248–254.
Correa-Freire, M. C., Freire, E., Barenholz, Y., Biltonen, R. L., & Tompson, T. E. (1979) *Biochemistry 18*, 442–445.
Cortese, J. D., & Frieden, C. (1990) *Cell Motil. Cytoskel. 17*, 236–249.
Cortese, J. D., Schwab, B. III, Frieden, C., & Elson, E. L. (1989) *Proc. Natl. Acad. Sci. U.S.A. 86*, 5773–5777.
Dietrich, C., Goldmann, W. H., Sackmann, E., & Isenberg, G. (1993) *FEBS Lett. 324*, 37–40.
Draeger, A., Amos, W. B., Ikebe, M., & Small, J. V. (1990) *J. Cell Biol. 111*, 2463–2473.

Fritz, M., Zimmermann, R. M., Bärmann, M., & Gaub, H. E. (1993) *Biophys. J. 65*, 1878–1885.
Furuhashi, K., Inagaki, M., Hatano, S., Fukami, K., & Takenawa, T. (1992) *Biochem. Biophys. Res. Commun. 184*, 1261–1265.
Goldmann, W. H., & Isenberg, G. (1993) *FEBS Lett. 336*, 408–410.
Goldmann, W. H., Niggli, V., Kaufmann, S., & Isenberg, G. (1992) *Biochemistry 31*, 7665–7671.
Goldmann, W. H., Käs, J., Sackmann, E., & Isenberg, G. (1993) *Biochem. Soc. Trans. 21*, 133S.
Graham, D. E., & Philips, M. C. (1979) *J. Colloid Interface Sci. 70*, 403–439.
Hartwig, J. H., & Stossel, T. P. (1975) *J. Biol. Chem. 250*, 5696–5705.
Hartwig, J. H., & Stossel, T. P. (1979) *J. Mol. Biol. 134*, 539–553.
Hartwig, J. H., & Stossel, T. P. (1981) *J. Mol. Biol. 145*, 563–581.
Hartwig, J. H., & Shevlin (1986) *J. Cell Biol. 103*, 1007–1020.
Heise, H., Bayerl, T., Isenberg, G., & Sackmann, E. (1991) *Biochim. Biophys. Acta 1061*, 121–131.
Heyn, S. P., Tilmann, R. W., Egger, M., & Gaub, H. E. (1991) *J. Biochem. Biophys. Methods 22*, 145–158.
Hope, M. J., Bally, M. B., Webb, G., & Cullis, P. R. (1985) *Biochim. Biophys. Acta 812*, 55–65.
Isenberg, G. (1991) *J. Muscle Res. Cell Motil. 12*, 136–144.
Isenberg, G., & Goldmann, W. H. (1992) *J. Muscle Res. Cell Motil. 13*, 587–589.
Isenberg, G., & Goldmann, W. H. (1995) in *The Cytoskeleton* (Hesketh, J. E., & Pryme, I. F., Eds.) Vol. I, JAI Press Inc., Greenwich, CT (in press).
Janmey, P. (1994) *Annu. Rev. Physiol. 56*, 169–191.
Jockusch, B. M., & Isenberg, G. (1981) *Proc. Natl. Acad. Sci. U.S.A. 78*, 3005–3009.
Kaufmann, S., Käs, J., Goldmann, W. H., Sackmann, E., & Isenberg, G. (1992) *FEBS Lett. 314*, 203–205.
Koteliansky, V. E., Glukhova, M. A., Shirinsky, V. P., Smirnov, V. N., Bushueva, T. L., Filimonov, V. V., & Venyaminov, S. Y. (1982) *Eur. J. Biochem. 121*, 553–559.
Laemmli, U. K. (1970) *Nature (London) 227*, 680–685.
Lentz, B. R., Clubb, K. W., Alford, D. R., Höchli, M., & Meissner, G. (1985) *Biochemistry 24*, 433–442.
Lentz, B. R., Carpenter, T. J., & Alford, D. R. (1987) *Biochemistry 26*, 5389–5397.
Lösche, M., Sackmann, E., & Möhwald, H. (1983) *Ber. Bunsen-Ges. Phys. Chem. 87*, 848.
McElhaney, R. N. (1986) *Biochim. Biophys. Acta 864*, 361–421.
Niggli, V., Dimitrow, D. P., Brunner, J., & Burger, M. M. (1986) *J. Biol. Chem. 261*, 6912–6918.
Nunnally, M. H., Powell, L. D., & Craig, S. W. (1981) *J. Biol. Chem. 256*, 2083–2086.
Parente, R. A., & Lentz, B. R. (1984) *Biochemistry 23*, 2353–2362.
Schullery, S. E., Schmidt, C. F., Felgner, P., Tillack, T. W., & Thompson, T. E. (1980) *Biochemistry 19*, 3919–3923.
Seils, J., Jockusch, B. M., & Dorfmüller, T. (1990) *Biopolymers 30*, 677–689.
Shizuta, Y., Shizuta, H., Gallo, M., Davies, P., Pastan, I., & Lewis, M. C. (1976) *J. Biol. Chem. 251*, 6562–6567.
Small, J. V., Fürst, D. O., & De May, J. (1986) *J. Cell Biol. 102*, 210–220.
Tempel, M., Goldmann, W. H., & Isenberg, G. (1994) *FEBS Lett.* (in press).
Wallach, D., Davies, P. J. A., & Pastan, I. (1978) *J. Biol. Chem. 253*, 3328–3335.
Weber, T., & Brunner, J. (1994) *Biochemistry* (submitted for publication).
Weiss, R. M., & McConnel, H. M. (1984) *Nature 310*, 5972.
Wong, M., Anthony, F. H., Tillack, T. W., & Thompson, T. E. (1982) *Biochemistry 21*, 4126–4132.
Zhou, X., & Arthur, G. (1992) *J. Lipid Res. 33*, 1233–1236.